ISSN 1063-780X, Plasma Physics Reports, 2017, Vol. 43, No. 12, pp. 1189–1197. © Pleiades Publishing, Ltd., 2017.

SPACE PLASMA

Ion-Scale Excitations in a Strongly Coupled Astrophysical Plasma with Nuclei of Heavy Elements[1]

M. R. Hossen[a]*, S. A. Ema[b], and A. A. Mamun[c]

[a] *Department of General Educational Development, Daffodil International University, Sukrabad, Dhaka-1207, Bangladesh*

[b] *Department of EEE, Sonargaon University, Dhaka-1215, Bangladesh*

[c] *Department of Physics, Jahangirnagar University, Savar, Dhaka-1342, Bangladesh*

**e-mail: rasel.plasma@gmail.com*

Received September 26, 2016; in final form, February 6, 2017

Abstract—The linear and nonlinear propagation of ultrarelativistic and nonrelativistic analysis on modified ion-acoustic (MIA) waves in a strongly coupled unmagnetized collisionless relativistic space plasma system is carried out. Plasma system is assumed to contain strongly coupled nonrelativistic ion fluids, both nonrelativistic and ultrarelativistic degenerate electron and positron fluids, and positively charged static heavy elements. The restoring force is provided by the degenerate pressure of the electron and positron fluids, whereas the inertia is provided by the mass of ions. The positively charged static heavy elements participate only in maintaining the quasineutrality condition at equilibrium. The well-known reductive perturbation method is used to derive the Burgers and Korteweg–de Vries equations. Their shock and solitary wave solutions are numerically analyzed to understand the localized electrostatic disturbances. The basic characteristics of MIA shock and solitary waves are found to be significantly modified by the effects of degenerate pressures of electron, positron, and ion fluids, their number densities, and various charge state of heavy elements. The implications of our results to dense plasmas in compact astrophysical objects (e.g., nonrotating white dwarfs, neutron stars, etc.) are briefly discussed.

DOI: 10.1134/S1063780X17120029

1. INTRODUCTION

The study of linear and nonlinear behavior of electrostatic disturbances in electron–positron–ion (e-p-i) plasmas have become one of the most interesting theoretical studies in recent years. This interest is primarily due to the fact that such plasmas are ubiquitous to astrophysical compact objects [1–6]. The existence of e-p-i plasmas have been confirmed in the early universe [7], where the plasma processes have played an important role in the evolution of the universe. In present times, such plasma is assumed to exist in many astrophysical environments, viz. the inner regions of accretion disks surrounding black holes [8], active galactic nuclei [9], relativistic jets that stream from quasars and active galaxies [10, 11], pulsar magnetospheres [12], the solar atmosphere [13, 14], Van Allen radiation belts [15–17], etc. In the laboratory, the e-p-i plasma can be created via the mechanism of pair production or by injecting positrons into the electron–ion system [3, 4].

In a high-density strongly coupled astrophysical plasma, electron and positron fluids are degenerate and ions are strongly coupled because the ion Coulomb coupling parameter $\Gamma = (Z_i^2 q_i^2 / a_i k_B T_i) > 1$, where q_i is the charge of ions, a_i is the interion spacing, T_i is the ion temperature, and Z_i is the ion charge state, respectively [18]. The ions are strongly coupled to each other through their mutual Coulomb interaction because of their high charge density. When the coupling parameter $\Gamma \gg 1$, then the plasma system is said to be strongly coupled. When the mass and charge of ions are very high, then ion plasmas can also show the strongly coupled behavior. Many authors [19, 20] have also showed it experimentally. Generally, the constituents of plasmas are electrons, ions, and atoms or molecules. On the other hand, dusty (or complex) plasmas contain static mesoscopic (multiply charged) particles [21]. In some relatively massive white dwarfs, one can think of the presence of heavier element like iron within the stars. The heavy nuclei are mainly formed into the interiors of massive stars. When these stars contract to very high densities, matter in their interiors will cool and become degenerate under certain conditions. The formation of heavy elements begins in this state of degeneracy. When explosion occurs, part of the heavy elements distribute over the surrounding space and leave one or more stellar remnants in the form of white dwarfs [22]. The degenerate

[1] The article is published in the original.

electron number density in such a compact object is very high, e.g., in white dwarfs, the degenerate electron number density can be of the order of 10^{30} cm^{-3}, so that the electron Fermi energy is comparable to the electron mass energy [23–25]. It is important to note that the degeneracy feature, which is a fundamental aspect of ordinary solids, arises due to exclusion mechanism when the de Broglie thermal wave length $\lambda_B = h/(2\pi m_e k_B T)^{1/2}$ [26].

Chandrasekhar [27, 28] assumed that the core of white dwarfs contains pure helium (He^4) nuclei as heavy elements, but more than 70 years later, Koester [29] noticed that the core of white dwarfs contains carbon (C^{12}) or oxygen (O^{15}) nuclei as heavy elements and that the electron species is relativistically degenerate only within the inner core of the white dwarfs, but is nonrelativistically degenerate in their outer mantle [30]. The equation of state for degenerate electrons in such space environments and astrophysical objects are explained by Chandrasekhar [27] for two limits, named as nonrelativistic and ultrarelativistic limits. The degenerate electron pressure equation is given by Chandrasekhar [27, 28] as $P_e \propto n_e^{5/3}$ for nonrelativistic limit and $P_e \propto n_e^{4/3}$ for ultrarelativistic limit, where P_e is the degenerate electron pressure and n_e is the degenerate electron number density.

Many authors [31, 32] have already discussed how the basic features of normal ion-acoustic waves vary in the presence of dust grains and they named of such waves as dust-ion-acoustic (DIA) waves. But for astrophysical compact objects (i.e., white dwarfs, neutron star, etc.) having densities about a million or more times solid density, dust grains would not have a chance to exist. Some recent works [29, 30, 33] showed that the presence of heavy ions like, carbon, oxygen, etc., are predominant in such astrophysical compact objects. So, the effect of the heavy ions has to be taken into account, especially for astrophysical objects where the degenerate plasma pressure and heavy ions play an important role in the formation and stability of the existing waves. Therefore, in our present work, we have considered normal ion-acoustic waves in the presence of heavy ions and we like to call such propagation as modified ion-acoustic (MIA) waves. The MIA waves are, in fact, the acoustic type of waves in which (i) the inertia is provided by the ion mass and the restoring force is provided by the degenerate pressures of positrons and electrons and (ii) the frequency is much higher than the dust plasma frequency. On the other hand, the dust-acoustic (DA) waves are the acoustic type of waves in which (i) the inertia is provided by the dust mass and the restoring force is provided by the thermal pressure of positrons and electrons and (ii) the frequency is much lower than the ion plasma frequency.

Recently, for understanding the localized electrostatic perturbations in compact astrophysical objects like white dwarfs, a large number of theoretical investigations [34–56] have been made on the nonlinear propagation of ion-acoustic (IA), positron-acoustic (PA), and electron-acoustic (EA) waves by considering a degenerate dense plasma model that assumes weakly coupled nondegenerate ion fluids and degenerate nonrelativistic or ultrarelativistic electron fluids. All of these investigations, which have shown the existence of IA/PA/EA solitary and shock structures, are not valid for strongly coupled nondegenerate or degenerate ion fluids. The role of strong correlation among ions can be the source of dissipation (dispersion) and can be responsible for the formation of shock (solitary) structures in such compact astrophysical objects. Again, dense astrophysical quantum plasmas can be confined by stationary heavy ions. Therefore, the effect of the heavy elements has to be taken into account, especially for astrophysical observations (such as white dwarfs, neutron stars, black holes, etc), where the degenerate plasma pressure and heavy ions play an important role in the formation and stability of the existing waves.

None of the authors did not consider the effects of strongly correlated relativistic ions and various charge states of heavy elements which can significantly modify the propagation of MIA solitary and shock structures. To the best of our knowledge, the MIA waves in such considerable plasma system has never been addressed. Therefore, it is worthwhile to present a first study for the MIA shock and solitary waves where the degenerate plasma pressure, strongly coupled nonrelativistic ion fluids, both weakly coupled nonrelativistic and ultrarelativistic degenerate electron and positron fluids, and various charge states of heavy elements play a vital role.

2. THEORETICAL MODEL AND BASIC EQUATIONS

We consider the linear and nonlinear propagation of MIA waves in a strongly coupled degenerate plasma system whose constituents are nonrelativistic degenerate ions, both nonrelativistic and ultrarelativistic degenerate electron and positron fluids, and positively charged static heavy elements. Thus, the equilibrium condition reads $n_{i0} + n_{p0} + Z_h n_{h0} = n_{e0}$, where n_{s0} is the unperturbed number density of the species s (here, $s = i, e, p$ for positively charged ion, electron, and positron, respectively), Z_h is the number of light ions residing onto the heavy element surface. The dynamics of low-frequency nonlinear MIA waves in such a strongly coupled degenerate plasma system is governed by the well-known generalized viscoelastic hydrodynamic equations [57–60] consisting of the continuity and momentum equations,

$$\frac{\partial n_s}{\partial t} + \frac{\partial}{\partial x}(n_s u_s) = 0, \quad (1)$$

$$D_\tau\left[n_i\left(D_t u_i + \frac{\partial\phi}{\partial x}\right) + \mu_i k_B T_{\rm eff}\frac{K_1}{n_i}\frac{\partial n_i^\alpha}{\partial x}\right] = \eta_l\frac{\partial^2 u_i}{\partial^2 x}, \quad (2)$$

and by the generalized degenerate pressure equation for the electron and positron fluids,

$$n_e\frac{\partial\phi}{\partial x} - K_2\frac{\partial n_e^\gamma}{\partial x} = 0, \quad (3)$$

$$n_p\frac{\partial\phi}{\partial x} - K_2\frac{\partial n_p^\gamma}{\partial x} = 0. \quad (4)$$

The system of equations is closed by Poisson's equation

$$\frac{\partial^2\phi}{\partial x^2} = -\rho, \quad (5)$$

$$\rho = n_i - \beta n_e + \lambda n_p + Z_h\mu_h. \quad (6)$$

Here, n_s is the plasma number density of the species s (where $s = e,i,p$ for electron, ion, and positron, respectively) normalized by its equilibrium value n_{s0}, u_s is the plasma species fluid speed normalized by $C_{im} = (m_e c^2/m_i)^{1/2}$ (where m_e (m_i) is the electron (ion) rest mass and c is the speed of light in vacuum), ϕ is the electrostatic wave potential normalized by $m_e c^2/e$ (where e is the electron charge), the time variable (t) is normalized by $\omega_{pi} = (4\pi n_{i0}^2/m_i)^{1/2}$, the space variable ($r$) is normalized by $\lambda_m = (m_e c^2/4\pi n_{s0}^2)^{1/2}$, $D_\tau = 1 + \tau_m\partial/\partial t$ (where τ_m is the viscoelastic relaxation time), $D_t = \partial/\partial t + u_i\partial/\partial x$, and $T_{\rm eff} = (\mu_i T_i + T_*)$ is the effective ion temperature. The latter consists of two parts, one (T_*) arising from the electrostatic interaction among strongly correlated positive ions and other ($\mu_i T_i$) arising from the ion thermal pressure. Again, $\eta = (\omega_{pi}/m_i n_{i0}\lambda_{Di}^2)[\eta_t + (4/3)\xi_t]$ is the normalized longitudinal viscosity coefficient, where η_t and ξ_t are the transport coefficients of shear and bulk viscosities. The parameter $\beta = n_{e0}/n_{i0}$ is the electron-to-ion number density ratio, $\lambda = n_{p0}/n_{i0}$ is the positron-to-ion number density ratio, and $\mu_h = n_{h0}/n_{i0}$ is the heavy ion-to-ion number density ratio. We have defined $K_1 = n_{i0}^{\alpha-1}K_i/m_i{}^2C_i{}^2$ and $K_2 = n_{e0}^{\gamma-1}K_e/m_i C_i{}^2 = n_{p0}^{\gamma-1}K_e/m_i C_i{}^2$. There are various approaches for calculating the ion transport coefficients, similar to those of one-component strongly coupled plasmas [57, 61, 62]. For our purposes, the parameter T_* (which arises from the electrostatic interactions among strongly correlated positive ions), viscoelastic ion relaxation time τ_m, and ion compressibility μ_i are written as [57]

$$T_* = \frac{N_{nn}}{3}\frac{Z_i^2 e^2}{a_i k_B}(1+\kappa)\exp^{-\kappa}, \quad (7)$$

$$\tau_m = \eta_l\frac{T_e}{T_{\rm eff}}\left[1 - \mu_i + \frac{4}{15}u(\Gamma)\right]^{-1}, \quad (8)$$

where N_{nn} is determined by the ion structure and corresponds to the number of nearest neighbors (viz., in crystalline state, $N_{nn} = 8$ for a body centered cubic lattice, $N_{nn} = 12$ for face centered cubic lattice, etc.); $\kappa = a_i/\lambda_{Di}$, with λ_{Di} being Thomas–Fermi screening length; and $u(\Gamma)$ is a measure of the excess internal energy of the system and is calculated for weakly coupled plasmas ($\Gamma < 1$) as $u(\Gamma) \simeq -(\sqrt{3}/2)\Gamma^{3/2}$. We can express $u(\Gamma)$ in terms of Γ for a range of $1 < \Gamma < 100$ [62] deriving an analytical relation

$$u(\Gamma) \simeq -0.89\Gamma + 0.95\Gamma^{1/4} + 0.19\Gamma^{-1/4} - 0.81, \quad (9)$$

where a small correction term due to finite number of particles is neglected. The dependence of the other transport coefficient η_l on Γ is somewhat more complex and cannot be expressed in such a closed analytical form. However, tabulated/graphical results of their functional behavior derived from the molecular dynamic simulations and a variety of statistical schemes are also available in literature [57].

3. FORMULATION OF LINEAR DISPERSION RELATIONS

The relation between the wave frequency ω and wave number k is known as the dispersion relation. To analyze the characteristics of linear waves, we derive the linear dispersion relation for the plasma system under consideration here. First, we consider perturbations varying as $e^{i(kx-\omega t)}$ in the small-amplitude limit and then by expanding the dependent variables in Eqs. (1)–(5) in a power series of ϵ, as described below in Eqs. (17)–(21), with the terms containing ϵ^2 or higher neglected and by replacing $\partial/\partial t \to -i\omega$ and $\partial/\partial x \to ik$, we get

$$\omega^2 + i\omega\eta k^2 = k^2\beta_1, \quad (10)$$

where $\beta_1 = \dfrac{K_2' + \mu_i k_B T_{\rm eff}K_1'(\lambda - \beta + Z_h\mu_h + 2)}{\lambda - \beta + Z_h\mu_h + 2}$. Now we separate the dispersion relation into its real and imaginary parts by setting $\omega = \omega_R + i\omega_I$; then, we obtain $\omega_R^2 - \omega_I^2 - \omega_I\eta k^2 = k^2\beta_1$ and $\omega_R(2\omega_I + \eta k^2) = 0$ for the real and the imaginary parts, respectively. For nonzero real frequency, the imaginary part reduces to $\omega_I = -k^2\eta/2$. This reflects the energy dissipation

associated with viscosity. Substituting $\omega_I = -k^2\eta/2$, we get the real angular frequency as

$$\omega_R = \sqrt{k^2\beta_1 - k^4\eta^2/4}. \quad (11)$$

We first consider the nondissipative case, i.e., ($\eta = 0$), which leads to the dispersion relation $\omega^2 = k^2\beta_1 \equiv \omega_0^2$ (for shock wave). Then, we consider the cases with $\eta = 0.4$ and 0.8.

To evaluate the linear characteristics of MIA solitary waves by linearizing the Eqs. (1)–(5), we obtain the linear dispersion relation in the form

$$\omega^2 = \frac{k^2 C_1}{k^2 + C}, \quad (12)$$

where, $C_1 = K_2' + \mu_i k_B T_{\text{eff}} K_1'(\lambda - \beta + Z_h\mu_h + 2)$ and $C = \lambda - \beta + Z_h\mu_h + 2$. In case of large wavelength (i.e., for $k \ll C$), the MIA solitary waves frequency is given by

$$\omega^2 = C_1\frac{k^2}{C}, \quad (13)$$

and the phase velocity of the MIA reads $\omega/k = (C_1/C)^{1/2}$ or

$$V_p = \sqrt{\frac{K_2' + \mu_i k_B T_{\text{eff}} K_1'(\lambda - \beta + Z_h\mu_h + 2)}{\lambda - \beta + Z_h\mu_h + 2}}. \quad (14)$$

It is seen that the linear dispersion relation for the MIA waves is significantly modified by the effects of adiabaticity, nonextensivity of electrons, and Maxwellian light ions.

4. FORMULATION OF NONLINEAR EQUATIONS

4.1. Derivation of the Burgers Equation

Now, we derive a dynamical equation for the nonlinear propagation of the MIA shock waves by using Eqs. (1)–(5). We employ a reductive perturbation technique to examine electrostatic perturbations propagating in the relativistic degenerate dense plasma due to the effect of dissipation and introduce the stretched coordinates [63]

$$\zeta = \epsilon(x - V_p t), \quad (15)$$

$$\tau = \epsilon^2 t, \quad (16)$$

where $V_p = \omega/k$ is the wave phase speed (with ω being angular frequency and k being the wave number of the perturbation mode) and ϵ is a smallness parameter measuring the weakness of dissipation ($0 < \epsilon < 1$). We then expand n_i, n_e, u_i, and ϕ, in power series of ϵ,

$$n_i = 1 + \epsilon n_i^{(1)} + \epsilon^2 n_i^{(2)} + \cdots, \quad (17)$$

$$n_e = 1 + \epsilon n_e^{(1)} + \epsilon^2 n_e^{(2)} + \cdots, \quad (18)$$

$$n_p = 1 + \epsilon n_p^{(1)} + \epsilon^2 n_p^{(2)} + \cdots, \quad (19)$$

$$u_i = \epsilon u_i^{(1)} + \epsilon^2 u_i^{(2)} + \cdots, \quad (20)$$

$$\phi = \epsilon\phi^{(1)} + \epsilon^2\phi^{(2)} + \cdots, \quad (21)$$

and develop equations in various powers of ϵ. To the lowest order in ϵ, using Eqs. (15)–(21), as well as Eqs. (1)–(5), we get $u_i^{(1)} = V_p\phi^{(1)}/(V_p^2 - \mu_i k_B T_{\text{eff}} K_1')$; $n_i^{(1)} = \phi^{(1)}/(V_p^2 - \mu_i k_B T_{\text{eff}} K_1')$; $n_e^{(1)} = n_p^{(1)} = \phi^{(1)}/K_2'$; and the phase speed

$$V_p = \left(\frac{K_2'}{\lambda - \beta + Z_h\mu_h + 2} + \mu_i k_B T_{\text{eff}} K_1'\right)^{1/2},$$

which is the same as we have obtained in case of linear waves.

We are interested in studying the nonlinear propagation of these dissipative MIA type electrostatic waves in a strongly coupled degenerate plasma. To the next higher order in ϵ, we obtain a set of equations

$$\frac{\partial n_s^{(1)}}{\partial\tau} - V_p\frac{\partial n_s^{(2)}}{\partial\zeta} - \frac{\partial}{\partial\zeta}[u_s^{(2)} + n_s^{(1)}u_s^{(1)}] = 0, \quad (22)$$

$$\frac{\partial u_i^{(1)}}{\partial\tau} - V_p\frac{\partial u_i^{(2)}}{\partial\zeta} + u_i^{(1)}\frac{\partial u_i^{(1)}}{\partial\zeta} + \frac{\partial\phi^{(2)}}{\partial\zeta} + \mu_i k_B T_{\text{eff}} K_1'\frac{\partial}{\partial\zeta}\left[n_i^{(2)} + \frac{(\alpha - 2)}{2}(n_i^{(1)})^2\right] - \eta\frac{\partial^2 u_i^{(1)}}{\partial\zeta^2} = 0, \quad (23)$$

$$\frac{\partial\phi^{(2)}}{\partial\zeta} - K_2'\frac{\partial}{\partial\zeta}\left[n_e^{(2)} + \frac{(\gamma - 2)}{2}(n_e^{(1)})^2\right] = 0, \quad (24)$$

$$\frac{\partial\phi^{(2)}}{\partial\zeta} - K_2'\frac{\partial}{\partial\zeta}\left[n_p^{(2)} + \frac{(\gamma - 2)}{2}(n_p^{(1)})^2\right] = 0, \quad (25)$$

$$\beta n_e^{(2)} - n_i^{(2)} - \lambda n_p^{(2)} = 0. \quad (26)$$

Now, combining Eqs. (22)–(26), we deduce the Burgers equation

$$\frac{\partial\phi^{(1)}}{\partial\tau} + A\phi^{(1)}\frac{\partial\phi^{(1)}}{\partial\zeta} = B\frac{\partial^2\phi^{(1)}}{\partial\xi^2}, \quad (27)$$

where the value of β and σ are given by

$$A = \frac{(V_p^2 - \mu_i k_B T_{\text{eff}} K_1')^2}{2V_p} \times\left[\frac{3V_p^2 + \mu_i k_B T_{\text{eff}} K_1'(\alpha - 2)}{(V_p^2 - \mu_i k_B T_{\text{eff}} K_1')^3} + \frac{(\gamma - 2)(\beta - \lambda)}{K_2'^2}\right], \quad (28)$$

$$B = \frac{\eta_I}{2}. \quad (29)$$

4.2. Derivation of the Korteweg–de Vries Equation

In order to search the Korteweg–de Vries (KdV) equation, we have to introduce first the stretched coordinates [63]

$$\xi = \epsilon^{1/2}(x - V_p t), \quad \tau = \epsilon^{3/2} t, \tag{30}$$

where ϵ and V_p are the same as before. We can expand the perturbed quantities n_i, u_i, and ϕ about the equilibrium values in power series of ϵ as for the Burgers equation. To the lowest order in ϵ, i.e., taking the coefficients of $\epsilon^{3/2}$ from both sides of Eqs. (17)–(20) and $\epsilon^{1/2}$ from both sides of Eq. (21), one can obtain the $n_i^{(1)}$, $u_i^{(1)}$, and V_p, which are exactly same what we have obtained from the Burgers equation.

To the next higher order in ϵ, i.e. taking the coefficients of $\epsilon^{5/2}$ from both sides of Eqs. (17)–(20), and ϵ^2 from both sides of Eq. (21), one can obtain another set of coupled equations for $n_i^{(2)}$, $u_i^{(2)}$, and $\phi^{(2)}$, which, along with the first set of coupled linear equations for $n_i^{(1)}$, $u_i^{(1)}$, and $\phi^{(1)}$, make a system of nonlinear equations. After some algebraic calculations, we obtain the nonlinear equation in the form

$$\frac{\partial \phi^{(1)}}{\partial \tau} + A\phi^{(1)}\frac{\partial \phi^{(1)}}{\partial \xi} + G\frac{\partial^3 \phi^{(1)}}{\partial \xi^3} = 0. \tag{31}$$

Equation (31) is known as the KdV equation, where the nonlinear coefficient A gives same value as for the Burgers equation and the dispersion coefficient G is given by

$$G = \frac{(V_p^2 - \mu_i k_B T_{\text{eff}} K_1')^2}{2V_p}. \tag{32}$$

5. PARAMETRIC INVESTIGATIONS AND RESULTS

The stationary shock wave solution of Burgers equation (27) is obtained by transforming the independent variables to $\xi = \zeta - U_0\tau'$ and $\tau' = \tau$, where u_0 is the speed of the shock waves, and imposing the appropriate boundary conditions, viz. $\phi^{(1)} \to 0$, $d\phi^{(1)}/d\xi \to 0$, and $d^2\phi^{(1)}/d\xi^2 \to 0$ at $\xi \to \pm\infty$. Thus, one can express the stationary shock wave solution of Burgers equation (27) as

$$\phi^{(1)} = \phi_m[1 - \tanh(\xi/\delta)], \tag{33}$$

where the amplitude ϕ_m and the width δ are given by

$$\phi_m = u_0/A, \tag{34}$$

$$\delta = 2B/u_0. \tag{35}$$

Table 1. Approximate ranges of the plasma parameters used in this investigation [64, 65]

Parameter	Parameter range
β	0.1–0.5
α	0.1–0.7
μ_h	0.1–0.45
η	0.1–0.8
u_0	0.1–1

The stationary solitary wave solution for KdV equation (31) is given by

$$\phi^{(1)} = \phi_m \text{sech}^2\left(\frac{\xi}{\Delta}\right), \tag{36}$$

where $\phi_m = 3u_0/A$ and $\Delta = (4G/u_0)^{1/2}$.

The ranges of the plasma parameters used to study the properties of shock and solitary structures are given in Table 1.

5.1. Linear Properties

The variation of the wave frequency ω with wave vector k for different values of the viscosity coefficient η is shown in Fig. 1, where the upper and lower curves correspond to the real (positive) and imaginary (negative) parts of the linear dispersion relation for MIA shock waves, respectively. It is observed that the real part of the wave frequency decreases (in absolute magnitude), while the imaginary part of the wave frequency increases (in absolute magnitude) with the increasing values of the viscosity coefficient (i.e., dissipative effect) η (see Fig. 1). Figure 2 illustrates the variation of the wave frequency ω with wave vector k for different values of heavy elements charge states Z_h. It is observed that the wave frequency decreases with the increasing values of heavy elements charge states Z_h.

5.2. Nonlinear Properties

5.2.1. Role of electron-to-ion number density ratio (via β). The effect of electron-to-ion number density ratio β on the shock and solitary profiles is illustrated in Figs. 3 and 4 for both nonrelativistic and ultrarelativistic limits. From Figs. 3 and 4, it is observed that the amplitudes of shock and solitary structures increase with increasing values of β. Physically, this happens due to the reason that it decreases the nonlinearity coefficient A. It is also observed that the amplitude of this shock and solitary waves are higher for the nonrelativistic case than for the ultrarelativistic case.

5.2.2. Role of positron-to-ion number density ratio (via λ). The effect of positron-to-ion number density ratio on the shock and solitary profiles is illustrated in Figs. 5 and 6 for both nonrelativistic and ultrarelativis-

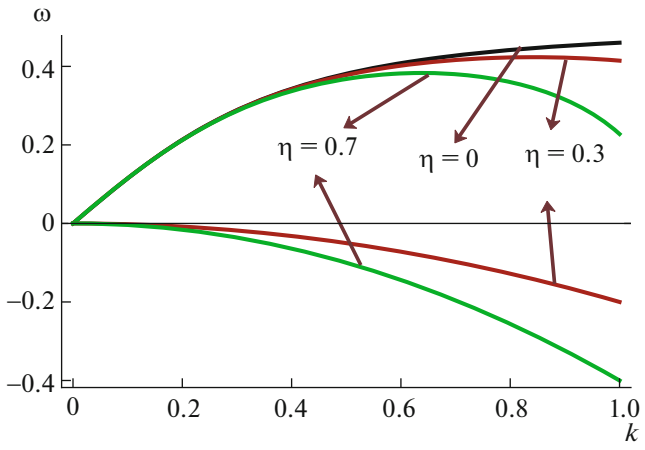

Fig. 1. (Color online) Variation of the wave frequency ω with the wave vector k for $\alpha = \gamma = 5/3$, $\beta = 0.3$, $\lambda = 0.4$, and $\mu_h = 0.3$ of the MIA shock waves linear dispersion relation. The upper (positive ω) curves are for the real part and the lower (negative ω) curves are for imaginary part of the MIA shock wave linear dispersion relation.

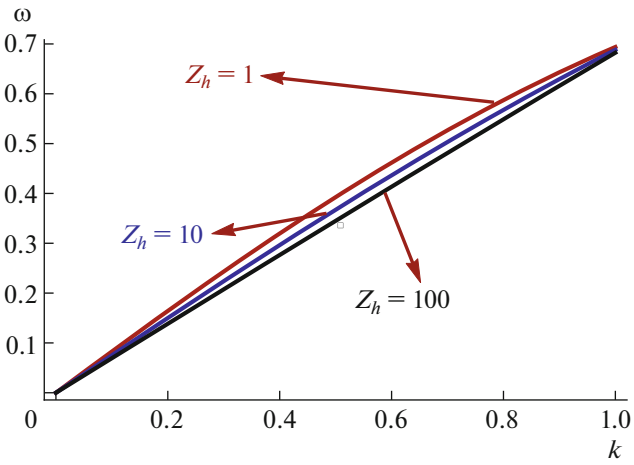

Fig. 2. (Color online) Variation of the wave frequency ω with the wave vector k for $\alpha = \gamma = 5/3$, $\beta = 0.3$, $\lambda = 0.4$, and $\mu_h = 0.3$ of the MIA solitary wave linear dispersion relation.

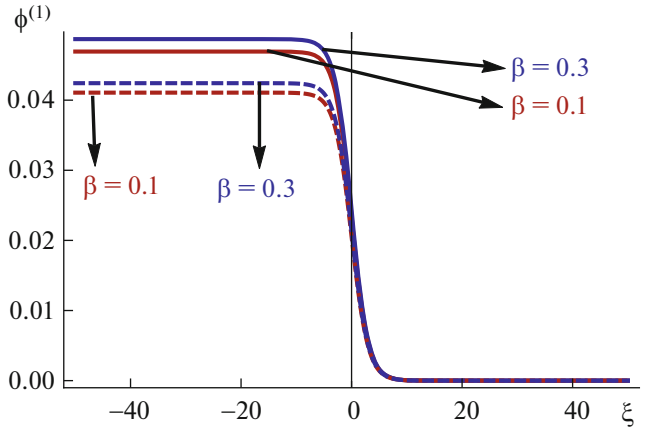

Fig. 3. (Color online) Variation of shock waves with ξ for different values of β. The solid and dashed curves correspond to the nonrelativistic and ultrarelativistic cases, respectively.

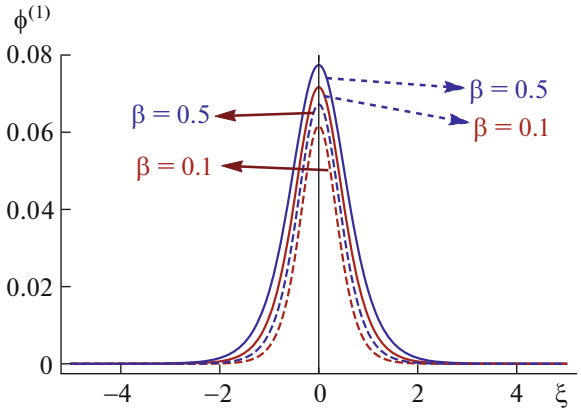

Fig. 4. (Color online) Variation of solitary waves with ξ for different values of β. The solid and dashed curves correspond to the nonrelativistic and ultrarelativistic cases, respectively.

tic limits. It is found that the amplitudes of the shock and solitary structures decrease with increasing values of λ. It happens on the basis of the driving force of the MIA wave, as the driving force for the MIA wave is provided by the ion inertia. Actually, an increase in the ion concentration (depopulation of electrons) causes a decrease in the driving force, which is provided by the ion inertia and, consequently, shock and solitary waves enervate. It is also found that the amplitude of these shock and solitary structures are distinctly higher for the nonrelativistic case than for the ultrarelativistic case.

5.2.3. Role of heavy ion-to-ion number density ratio (via μ_h). Figures 7 and 8 illustrate the effect of heavy ion-to-ion number density ratio on the amplitudes of the MIA shock and solitary structures. It is found that the amplitudes of shock and solitary structures decrease with increasing values of μ_h. Physically, this happens due to the reason that it decreases the phase speed of the MIA waves (see expression for V_p).

5.2.4. Kinematic viscosity effect (via η). The amplitudes of the shock and solitary structures also depend on the kinematic viscosity coefficient η. It is observed that the amplitudes of both shock and solitary structures decrease with increasing values of η. Physically,

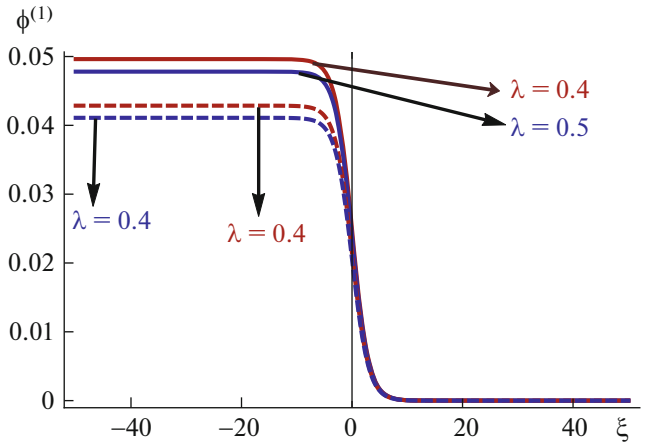

Fig. 5. (Color online) Variation of shock waves with ξ for different values of λ. The solid and dashed curves correspond to the nonrelativistic and ultrarelativistic cases, respectively.

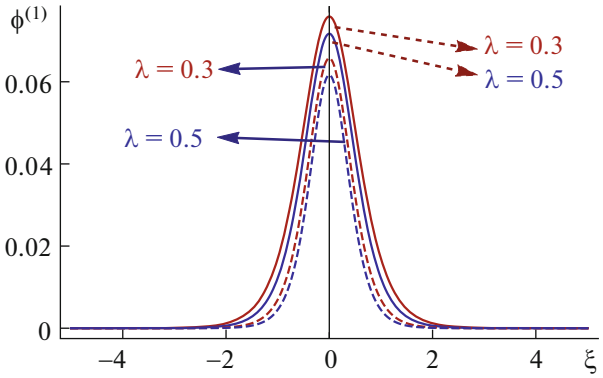

Fig. 6. (Color online) Variation of solitary waves with ξ for different values of λ. The solid and dashed curves correspond to the nonrelativistic and ultrarelativistic cases, respectively.

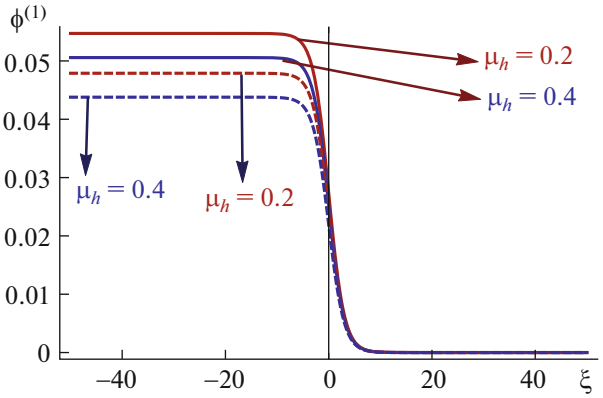

Fig. 7. (Color online) Variation of shock waves with ξ for different values of μ_h. The solid and dashed curves correspond to the nonrelativistic and ultrarelativistic cases, respectively.

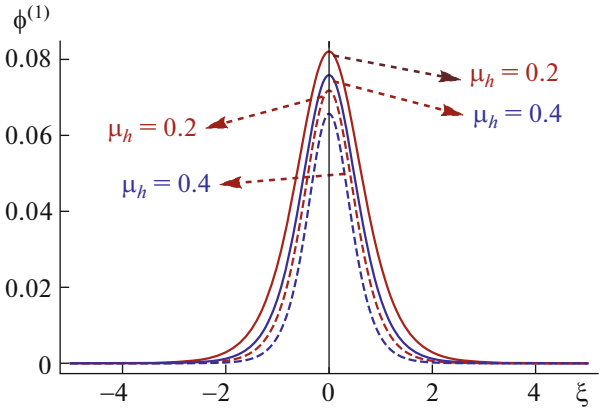

Fig. 8. (Color online) Variation of solitary waves with ξ for different values of μ_h. The solid and dashed curves correspond to the nonrelativistic and ultrarelativistic cases, respectively.

this happens due to the reason that it increases the dissipative constant B. The effect of kinematic viscosity on the linear dispersion relation for MIA shock waves was already discussed in Section 5.1.

5.2.5. Relativistic effects. The properties of shock and solitary wave are significantly affected by the relativistic effects, which manifest themselves through the adiabatic exponents α and gamma γ. There are two relativistic limits called nonrelativistic ($\alpha = \gamma = 5/3$) and ultrarelativistic ($\alpha = 5/3$, $\gamma = 4/3$), which significantly modify the shock and solitary profiles. It is found that the amplitudes of the shock and solitary structures are higher for the nonrelativistic case than for the ultrarelativistic case.

5.2.6. Role of heavy elements charge states. The amplitude of solitary and shock structures are significantly modified by the various charge states of heavy elements. Figures 9 and 10 illustrate the variation of the amplitudes of shock and solitary structures with ξ for different values of Z_h. It is observed that the amplitudes of the shock and solitary structures decrease with increasing values of Z_h. The linear dispersion relation, i.e., ω versus k graph (see Fig. 1) of the MIA solitary waves also drastically affected by the various charge states of heavy ions. From Fig. 1, it is observed that the phase speed of the MIA waves also decreases with increasing values of Z_h.

It is also important to note here that, when the dispersion (dissipation) effect is much more pronounced than the dissipation (dispersion) effect, and the dissipation (dispersion) effect is neglected, strongly coupled degenerate dense plasmas support solitary

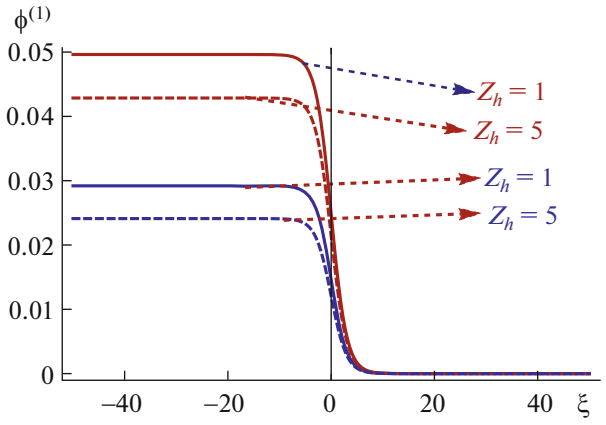

Fig. 9. (Color online) Variation of shock waves with ξ for different values of Z_h. The solid and dashed curves correspond to the nonrelativistic and ultrarelativistic cases, respectively.

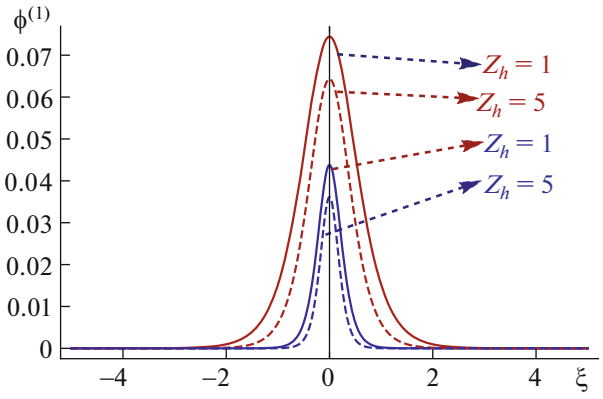

Fig. 10. (Color online) Variation of solitary waves with ξ for different values of Z_h. The solid and dashed curves correspond to the nonrelativistic and ultrarelativistic cases, respectively.

(shock) waves. To neglect the effect of the MIA dispersion in comparison with that of the dissipation, or vice versa, one has to choose a suitable scaling (stretching of coordinates), such as the one that we used in our investigation of the MIA shock and solitary waves. To investigate only solitary wave propagation in dusty or normal plasma system, it is not important to take viscosity term [66–68] in the momentum equation; however, for describing both solitary and shock wave characteristics, the viscosity term is essential to form the shock wave structures.

6. DISCUSSION

In this manuscript, we have presented a rigorous theoretical investigation of the nonlinear propagation of MIA shock and solitary structures in a strongly coupled unmagnetized collisionless degenerate plasma containing relativistic electron and positron fluids, nonrelativistic inertial ions, and positively charged static heavy elements. We have derived the Burgers and KdV equations by using the reductive perturbation method, and numerically analyzed their solitary and shock profiles. It is observed that the plasma system under consideration supports MIA shock and solitary structures, whose basic properties are found to be significantly modified due to the plasma particle number densities. Our results also show how the presence of ions of the heavier elements, C or O (instead of He), can modify the basic features of MIA waves.

To conclude, it may be stressed here that our present investigation would be useful to study the effects of degenerate pressure in interstellar and space plasmas [69–71], in particular, in stellar polytropes [72], hadronic matter and quark–gluon plasma [73], proto-neutron stars [74], dark-matter halos [75], etc., as well as laboratory plasmas [3, 4] in which nonrelativistic strongly coupled degenerate ions, both nonrelativistic and ultrarelativistic weakly coupled degenerate electron and positron fluids, and positively charged static heavy elements are the dominant plasma species.

ACKNOWLEDGMENTS

M.R. Hossen and S.A. Ema gratefully acknowledge Ministry of National Science and Technology, Bangladesh, for the M.S. research fellowship.

REFERENCES

1. M. C. Begelman, R. D. Blanford, and M. J. Rees, Rev. Mod. Phys. **56**, 255 (1984).
2. M. Tribeche, K. Aoutou, S. Younsi, and R. Amour, Phys. Plasmas **16**, 072103 (2009).
3. R. G. Greaves and C. M. Surko, Phys. Plasmas **4**, 1528 (1997).
4. P. Helander and D. J. Ward, Phys. Rev. Lett. **90**, 135004 (2003).
5. S. Ali, W. M. Moslem, P. K. Shukla, and R. Schlickeiser, Phys. Plasmas **14**, 082307 (2007).
6. W. M. Moslem, I. Kourakis, P. K. Shukla, and R. Schlickeiser, Phys. Plasmas **14**, 102901 (2007).
7. M. J. Rees, in *The Very Early Universe,* Ed. by G. W. Gibbons, S. W. Hawking, and S. Siklas (Cambridge University Press, Cambridge, 1983), p. 29.
8. W. H. Lee, E. Ramirez-Ruiz, and D. Page, Astrophys. J. **632**, 421 (2005).
9. H. R. Miller and P. J. Witta, *Active Galactic Nuclei* (Springer-Verlag, Berlin, 1987), p.202.
10. V. V. Zheleznyakov and S. A. Koryagin, Astron. Lett. **28**, 727 (2002).
11. V. V. Zheleznyakov and S. A. Koryagin, Astron. Lett. **31**, 713 (2005).
12. F. C. Michel, Rev. Mod. Phys. **54**, 1 (1982).

13. E. Tandberg-Hansen and A. G. Emslie, *The Physics of Solar Flares* (Cambridge University Press, Cambridge, 1988), p.138.
14. B. Kozlovsky, R. J. Murphy, and G.H. Share, Astrophys. J. **604**, 892 (2004).
15. A. P. Lightman, Astrophys. J. **253**, 842 (1982).
16. A. A. Zdziarski, Astrophys. J. **335**, 786 (1987).
17. F. C. Michel, *Theory of Neutron Star Magnetosphere* (Chicago University Press, Chicago, 1991), p. 456.
18. P. K. Shukla, A. A. Mamun, and D. A. Mendis, Phys. Rev. E **84**, 026405 (2011).
19. A. Kumar, V. Sivakumaran, J. Ashwin, R. Ganesh, and H. C. Joshi, Phys. Plasmas **20**, 082708 (2013).
20. V. Fortov, I. Iakubov, and A. Khrapak, *Physics of Strongly Coupled Plasma* (Oxford University Press, Oxford, 2006).
21. W. D. Kraeft, Plasma Phys. Controlled Fusion **49**, 1111 (2007).
22. G. B. van Albada, Astrophys. J. **105**, 393 (1947).
23. A. A. Mamun and P. K. Shukla, Phys. Lett. A **324**, 4238 (2010).
24. M. R. Hossen, L. Nahar, S. Sultana, and A. A. Mamun, High Energy Density Phys. **13**, 13 (2014).
25. M. R. Hossen, L. Nahar, S. Sultana, and A. A. Mamun, Astrophys. Space Sci. **353**, 123 (2014).
26. W. F. El-Taibany and M. Wadati, Phys. Plasmas **14**, 103703 (2007).
27. S. Chandrasekhar, Astrophys. J. **74**, 81 (1931).
28. S. Chandrasekhar, Phil. Mag. **11**, 592 (1931).
29. D. Koester, Astron. Astrophys. **11**, 33 (2002).
30. P. K. Shukla and B. Eliasson, Phys. Usp. **53**, 51 (2010).
31. T. V. Losseva, S. I. Popel, and A. P. Golub, Plasma Phys. Rep. **38**, 729 (2012).
32. M. S. Zobaer, N. Roy, and A. A. Mamun, J. Mod. Phys. **3**, 755 (2012).
33. E. Garcia-Berro, S. Torres, L. G. Althaus, I. Renedo, P. Loren-Aguiltar, A. H. Corsico, R. D. Rohrmann, M. Salaris, and J. Isern, Nature **465**, 194 (2010).
34. A. Shah and R. Saeed, Phys. Lett. A **373**, 4164 (2009).
35. M. A. Hossen, M. R. Hossen, and A. A. Mamun, Braz. J. Phys. **44**, 703 (2014).
36. M. A. Hossen, M. R. Hossen, S. Sultana, and A. A. Mamun, Astrophys. Space Sci. **357**, 34 (2015).
37. M. R. Hossen, S. A. Ema, and A. A. Mamun, Commun. Theor. Phys. **62**, 888 (2014).
38. W. Masood, A. M. Mirza, and M. Hanif, Phys. Plasmas **15**, 072106 (2008).
39. M. R. Hossen, L. Nahar, and A. A. Mamun, Phys. Scr. **89**, 105603 (2014).
40. M. R. Hossen, L. Nahar, and A. A. Mamun, Braz. J. Phys. **44**, 638 (2014).
41. M. R. Hossen, L. Nahar, and A. A. Mamun, J. Astrophys. **2014**, 653065 (2014).
42. H. R. Pakzad, Canad. J. Phys. **89**, 961 (2011).
43. H. R. Pakzad and M. Tribeche, J. Fusion Energy **32**, 171 (2013).
44. M. A. Hossen, M. R. Hossen, and A. A. Mamun, J. Korean Phys. Soc. **65**, 1883 (2014).
45. M. G. Shah, M. R. Hossen, and A. A. Mamun, Braz. J. Phys. **45**, 219 (2015).
46. M. G. Shah, M. R. Hossen, S. Sultana, and A. A. Mamun, Chin. Phys. Lett. **32**, 085203 (2015).
47. M. G. Shah, M. R. Hossen, and A. A. Mamun, Chin. Phys. Lett. **81**, 905810517 (2015).
48. M. G. Shah, M. R. Hossen, and A. A. Mamun, J. Korean Phys. Soc. **66**, 1239 (2015).
49. S. A. Ema, M. R. Hossen, and A. A. Mamun, Contrib. Plasma Phys. **55**, 551 (2015).
50. B. Hosen, M. G. Shah, M. R. Hossen, and A. A. Mamun, Euro. Phys. J. Plus **131**, 81 (2016).
51. B. Hosen, M. Amina, A. A. Mamun, and M. R. Hossen, J. Korean Phys. Soc. **69**, 1762 (2016).
52. M. R. Hossen, L. Nahar, and A. A. Mamun, Braz. J. Phys. **44**, 673 (2014).
53. M. R. Hossen, L. Nahar, and A. A. Mamun, J. Korean Phys. Soc. **65**, 1863 (2014).
54. M. R. Hossen and A. A. Mamun, Braz. J. Phys. **45**, 200 (2015).
55. M. R. Hossen and A. A. Mamun, Plasma Sci. Technol. **17**, 177 (2015).
56. M. R. Hossen and A. A. Mamun, J. Korean Phys. Soc. **65**, 2045 (2015).
57. S. Ichimaru, H. Iyetomi, and S. Tanaka, Phys. Rep. **149**, 91 (1987).
58. A. A. Mamun, P. K. Shukla, and T. Farid, Phys. Plasmas **7**, 2329 (2000).
59. S. A. Ema, M. R. Hossen, and A. A. Mamun, Phys. Plasmas **22**, 092108 (2015).
60. S. A. Ema, M. R. Hossen, and A. A. Mamun, Contrib. Plasma Phys. **55**, 596 (2015).
61. S. Ichimaru and S. Tanaka, Phys. Rev. Lett. **56**, 2815 (1986).
62. W. L. Slattery, G. D. Doolen, and H. E. Dewitt, Phys. Rev. A **21**, 2087 (1980).
63. S. Maxon and J. Viecelli, Phys. Rev. Lett. **32**, 4 (1974).
64. W. F. El-Taibany and A. A. Mamun, Phys. Rev. E **85**, 026406 (2012).
65. W. F. El-Taibany, A. A. Mamun, and K. H. El-Shorbagy, Adv. Space Res. **50**, 101 (2012).
66. S. I. Popel, S. V. Vladimirov, and P. K. Shukla, Phys. Plasmas **2**, 716 (1995).
67. J. Srinivas, S. I. Popel, and P. K. Shukla, J. Plasma Phys. **55**, 209 (1996).
68. G. Lu, Y. Liu, Y. Wang, L. Stenflo, S. I. Popel, and M. Y. Yu, J. Plasma Phys. **76**, 267 (2010).
69. W. Masood and B. Eliasson, Phys. Plasmas **18**, 034503 (2011).
70. Ata-ur-Rahman, A. Mustaq, S. Ali, and A. Qamar, Commun. Theor. Phys. **59**, 479 (2013).
71. F. Ferro, A. Lavagno, and P. Quarati, Eur. Phys. J. A **21**, 529 (2004).
72. A. R. Plastino and A. Plastino, Phys. Lett. A **174**, 384 (1993).
73. G. Gervino, A. Lavagno, and D. Pigato, Cent. Eur. J. Phys. **10**, 594 (2012).
74. A. Lavagno and D. Pigato, Eur. Phys. J. A **47**, 52 (2011).
75. C. Feron and J. Hjorth, Phys. Rev. E **77**, 022106 (2008).